Earth's Future

RESEARCH ARTICLE
10.1029/2023EF004191

Natural Variability Can Mask Forced Permafrost Response to Stratospheric Aerosol Injection in the ARISE-SAI-1.5 Simulations

A. L. Morrison[1], **E. A. Barnes**[1], **and J. W. Hurrell**[1]

[1]Department of Atmospheric Sciences, Colorado State University, Fort Collins, CO, USA

Key Points:

- Projected natural variability in permafrost fields in peatland and Yedoma regions can mask forced response to stratospheric aerosol injection (SAI)
- Effect of SAI on active layer and soil temperature is only detectable after more than a decade of aerosol deployment
- Natural variability affects likelihood of reaching precursor to permafrost tipping point despite surface cooling effect of SAI

Supporting Information:

Supporting Information may be found in the online version of this article.

Correspondence to:

A. L. Morrison,
ariel.morrison@colostate.edu

Citation:

Morrison, A. L., Barnes, E. A., & Hurrell, J. W. (2024). Natural variability can mask forced permafrost response to stratospheric aerosol injection in the ARISE-SAI-1.5 simulations. *Earth's Future*, *12*, e2023EF004191. https://doi.org/10.1029/2023EF004191

Received 12 OCT 2023
Accepted 30 APR 2024

Abstract Stratospheric aerosol injection (SAI) has been proposed as a potential method for mitigating risks and impacts associated with anthropogenic climate change. One such risk is widespread permafrost thaw and associated carbon release. While permafrost has been shown to stabilize under different SAI scenarios, natural variability may mask this forced response and make it difficult to detect if and when SAI is stabilizing permafrost. Here we use the 10-member ensemble from the ARISE-SAI-1.5 simulations to assess the spread in projected active layer depth and permafrost temperature across boreal permafrost soils and specifically in four peatland and Yedoma regions. The forced response in active layer depth and permafrost temperature quickly diverges between an SAI and non-SAI world, but individual ensemble members overlap for several years following SAI deployment. We find that, due to projected permafrost variability, it may take more than a decade of SAI deployment to detect the effects of SAI on permafrost temperature and almost 30 years to detect its effects on active layer depth. Not only does natural variability make it more difficult to detect SAI's influence, it could also affect the likelihood of reaching a permafrost tipping point. In some realizations, SAI fails to prevent a local tipping point that is also reached in a non-SAI world. Our results underscore the importance of accounting for natural variability in assessments of SAI's potential influence on the climate system.

Plain Language Summary Injecting highly reflective particles into the upper atmosphere, or stratospheric aerosol injection (SAI), is a proposed climate intervention method for deliberately stabilizing or cooling the Earth's temperature and preventing undesirable impacts of human-caused climate change, such as thawing permafrost. Permafrost can potentially release stored carbon into the atmosphere as carbon dioxide and methane that contributes to the greenhouse effect. Climate model simulations show that SAI could stabilize permafrost and prevent it from thawing, but that natural fluctuations in the Earth's climate may cause a wide range of outcomes for future permafrost thaw depth and soil temperature. We show that, due to these natural climate fluctuations, it may take 10–30 years of SAI to clearly see its influence on permafrost thaw depth and temperature. Certain conditions that lead to runaway thaw and soil carbon release (i.e., tipping points) may also occur even if SAI successfully stabilizes the Earth's globally averaged temperature. When weighing possible outcomes of proposed climate intervention strategies, it is important to consider the effects of natural climate fluctuations in assessing the pros and cons of different strategies.

1. Introduction

Despite efforts to reduce greenhouse gas emissions and meet the climate goals of the 2015 Paris Agreement, humanity is not on track to limit warming to 1.5°C above pre-industrial temperatures (Matthews & Wynes, 2022; Pihl et al., 2019). Climate intervention, or deliberate manipulation of the Earth's climate, is gaining traction as a possible method for mitigating increasing temperatures as a result of anthropogenic activity. Stratospheric aerosol injection (SAI) is a form of solar climate intervention that aims to reduce incoming sunlight by injecting highly reflective sulfur dioxide (SO_2) particles into the stratosphere, in an effort to stabilize or reduce surface temperature. The National Academies of Sciences, Engineering, and Medicine (NASEM) recommended the formation of an international transdisciplinary research program to improve our understanding of the feasibility and consequences of solar climate intervention strategies (NASEM, 2021) in light of observed impacts already attributable to the current degree of warming (Gulev et al., 2021). These observed impacts are not evenly distributed across the globe: for example, the Arctic is warming several times faster than the global average (Rantanen et al., 2022), leading to concern that this warming may lead to tipping conditions that cause further runaway warming, and adding urgency to evaluating the global and regional impacts of different SAI methods.

While most proposed SAI methods do not specifically target the poles, different potential SAI strategies may be effective at stabilizing Arctic Ocean surface temperatures (Richter et al., 2022), maintaining Arctic sea ice extent near present-day values (Hueholt et al., 2023; Jones et al., 2018; Kravitz et al., 2019), and slowing the rate of boreal permafrost thaw (Chen et al., 2020, 2023; H. Lee et al., 2019; W. Lee et al., 2023; Liu et al., 2023; Morrison et al., 2024). The thawing of permafrost, or ground that is consistently frozen for at least two consecutive years, is a particular area of concern because of the carbon stored in permafrost soils. Recent estimates put the total carbon storage of boreal permafrost soils at 1,460–1,600 PgC (Hugelius et al., 2014; Schuur et al., 2015, 2018), or roughly twice the carbon stored in the atmosphere (Schuur et al., 2008). The type of permafrost soils affects the distribution of carbon. For example, peatlands contain a high density of organic material, but cover a relatively small area so overall account for about 12% of permafrost carbon (Hugelius et al., 2020). Yedoma, or Pleistocene-age ice-rich permafrost that can be more than 40 m thick (Miner et al., 2022; Strauss et al., 2021; Tarnocai et al., 2009), is not made of carbon-rich soils but is so deep that the total accumulated carbon inventory of Yedoma is estimated to be ∼20%–30% of the total boreal permafrost carbon stores (Schuur et al., 2018; Strauss et al., 2013, 2017). As permafrost temperatures increase and permafrost soils thaw, this stored carbon can be released into the atmosphere as CO_2 or CH_4.

Certain permafrost tipping conditions may be reached if permafrost thaws abruptly, releasing large amounts of this stored carbon, or setting off a positive feedback within the soil that accelerates the rate of thaw. Permafrost tipping conditions can be regional (i.e., accelerated localized thaw around the initial thaw area) or global (i.e., global temperature increase from ∼200 GtC release caused by complete permafrost collapse; Armstrong McKay et al., 2022). While permafrost tipping points can be difficult to quantify and the likelihood of reaching them is uncertain (Armstrong McKay et al., 2022; Lenton, 2012), particular conditions within permafrost soil make it more likely to reach tipping conditions. The formation of talik, a layer of thawed soil within permafrost, can thaw surrounding permafrost and accelerate in-ground respiration, which in turn can lead to more permafrost thaw and soil carbon release (Connon et al., 2018; Devoie et al., 2019; Parazoo et al., 2018). Taliks can also exist between permafrost and the base of the active layer, which is the ground layer that thaws and freezes each year. Devoie et al. (2019) found that permafrost can start to thaw in the same year that a talik forms, indicating that talik formation can initiate rapid permafrost thaw. If a talik survives through the winter, it is nearly impossible to refreeze that talik or the surrounding permafrost. Since talik formation can initiate a positive feedback of thawing and soil respiration, it may be considered a precursor to a permafrost tipping condition.

SAI has been proposed as a strategy to prevent widespread permafrost thaw, but there is uncertainty about how effective it might be and when we could detect its effects. It is especially uncertain given the range of scenarios in which SAI could be deployed, from stabilizing surface temperatures to rapidly cooling the planet (MacMartin et al., 2022). The response to solar climate intervention strategies can vary greatly in fields such as temperature and precipitation due to regional differences and natural variability within the climate system (Barnes et al., 2022; Dagon & Schrag, 2017; Labe et al., 2023; Ricke et al., 2010). Over short timescales, natural variability can mask a system's response to external forcings such as anthropogenic warming caused by greenhouse gas emissions (e.g., Deser et al., 2014), or anthropogenic cooling caused by SAI. This masking could hinder efforts to determine what, if any, effect SAI has on a system in the short term (Keys et al., 2022). Different SAI simulations have been shown to slow the rate of permafrost thaw (Chen et al., 2020, 2023; H. Lee et al., 2019; W. Lee et al., 2023) and prevent talik formation (Morrison et al., 2024) in the forced response. In a region as sensitive to temperature shifts as the Arctic, however, natural variability may lead to permafrost thaw or talik formation even if SAI successfully stabilizes global mean surface temperatures, thereby masking the forced response to SAI. Natural variability could also accelerate how quickly SAI halts permafrost thaw, essentially amplifying the forced response in preserving permafrost.

Large-scale solar climate intervention currently only exists in the realm of climate models that provide a range of possible future outcomes as a result of SAI deployment (e.g., Kravitz et al., 2011; Richter et al., 2022; Tilmes et al., 2018). Each possible outcome is represented by a single member of an “ensemble” of simulations. The ensemble mean (EM) defines the forced response to SAI deployment within that climate model. Our future will be a combination of the forced response and the influence of natural variability, so the real world can be thought of as a single ensemble member. No studies have yet assessed the effect of SAI on permafrost in the context of internal variability, nor has there been work on whether natural variability may mask the forced response of permafrost to certain SAI strategies. Using output from every ensemble member of an SAI deployment simulation, here we seek to answer three main questions:

1. What is the range of certain boreal permafrost responses to SAI due to natural variability, especially in regions with high organic soil matter content?
2. Given a possible range of permafrost responses to SAI due to natural variability, how long might it take to detect the effect of SAI on permafrost in a single climate realization?
3. How may natural variability affect the likelihood of reaching a precursor condition to permafrost tipping points?

2. Materials and Methods

2.1. Climate Intervention and Control Simulations

To explore the role of natural variability in the permafrost response to SAI, we use output from two parallel 10-member climate simulations. Both simulations were run with the fully-coupled Community Earth System Model version 2 (CESM2; Danabasoglu et al., 2020) at a ∼1° horizontal resolution grid. CESM2 uses the Whole Atmosphere Community Climate Model version 6 (WACCM6; Gettelman et al., 2019) as the atmospheric component, a modified version of the Parallel Ocean Program version 2 (POP2; Smith et al., 2010) as the ocean component, and the Community Land Model version 5 (CLM5; Lawrence et al., 2018, 2019) as the land component. WACCM6 has 70 vertical layers with a model top at 140 km to explicitly capture stratospheric processes, including stratospheric chemistry. CLM5 has 25 soil levels down to almost 50 m, with soil level thickness ranging from 0.4 cm to 8.5 m. Up to the first 20 layers are soil and at least the bottom five layers are bedrock. Bedrock depth is variable (Lawrence et al., 2018), but is no deeper than 8.6 m. The vertical resolution of the soil layers increased from previous versions of the land model in order to more accurately simulate hydrological and permafrost processes. CLM5 is biogeochemically active and includes vertically resolved soil carbon, which is mixed through the soil layers by bioturbation, cryoturbation, and diffusion. Soil carbon decomposition is controlled by temperature, moisture, and oxygen availability (Lawrence et al., 2019).

The non-SAI control simulation from CESM2 uses the Shared Socioeconomic Pathway 2–4.5 (SSP2-4.5; Riahi et al., 2017) emissions scenario. The SSP2-4.5 simulation has five members run from 2015 to 2069 and five members run from 2015 to 2100. The parallel simulation in which SAI is deployed is the Assessing Responses and Impacts of Solar climate intervention on the Earth system with Stratospheric Aerosol Injection 1.5 simulation (ARISE-SAI-1.5), which was designed and run by Richter et al. (2022) using CESM2. ARISE-SAI-1.5 runs from 2035 to 2069 and also utilizes the SSP2-4.5 emissions scenario. In the simulation, sulfur dioxide aerosols are injected into the stratosphere at ∼21.5 km from 15°/30°N/S at 180°E starting in 2035. A feedback-control algorithm (Kravitz et al., 2017; MacMartin et al., 2014) within the simulations adjusts the volume and altitude of aerosols deployed from each location in order to meet three climate targets: to maintain global mean surface temperatures close to 1.5°C above pre-industrial levels, to maintain the north–south surface temperature gradient, and to maintain the equator-to-pole surface temperature gradient (Richter et al., 2022). To meet these temperature goals, the largest amount of aerosol injection occurs at 15°S (6 Tg per year by 2069), and the smallest amount is injected at 30°N (nearly 0 Tg per year by 2069). The aerosols injected in the model affect surface temperature by blocking some incoming sunlight and do not change atmospheric CO_2 concentrations relative to the non-SAI simulations described above.

2.2. Permafrost Data and Talik Formation

In CESM2, permafrost exists in grid cells where there is a value for the ALTMAX variable, which is the annual maximum active layer depth. ALTMAX is the deepest thawed soil layer, and therefore the soil layers underneath the base of the active layer are frozen. The depth of the active layer can be 0 m if the entire subsurface column is permafrost. A grid cell contains permafrost soil if ALTMAX is shallower than the depth of the bedrock in that cell, which means that the active layer does not extend all the way to the bedrock and that some of the soil column is permafrost. To assess possible permafrost outcomes under SAI, we focus on changes to the annual mean active layer depth (ALT), ALTMAX, and annual mean soil temperature down to the bedrock in grid cells with permafrost (TSOI). TSOI is the weighted average of soil temperature in each layer from the bottom of the active layer to the top of the bedrock, where the depth of each layer is the weight.

We focus on ALT and ALTMAX because they are proxies for permafrost extent. A deeper active layer means the underlying permafrost is warmer and more degraded, and therefore is closer to thawing conditions. A deeper active layer also means more soil is exposed to microbial activity that releases stored carbon into the atmosphere through decomposition and respiration. We focus on TSOI because temperature directly informs us whether the

10.1029/2023EF004191

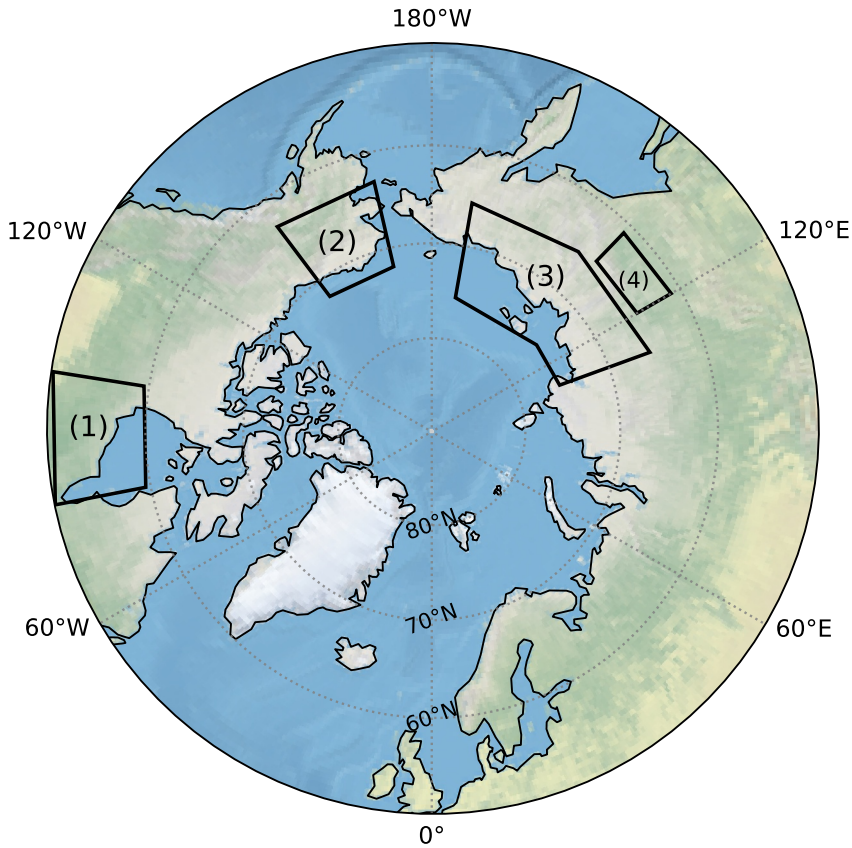

Figure 1. Map of regions selected to assess regional variability in permafrost fields. The boxed regions are (1) Canada peatland, (2) Alaska Yedoma, (3) Siberia Yedoma, and (4) Tibetan Plateau Yedoma.

upper soil levels are thawed. Most permafrost soil carbon is stored in the upper 3 m (Tarnocai et al., 2009), so thawing can potentially release much of the stored carbon. Increasing TSOI may also inform us whether permafrost is warming and degrading even if the active layer depth has not yet changed. There is an established relationship between mean annual air temperature and mean annual ground temperature (Burke et al., 2020), so the surface cooling effects of SAI may also influence in-ground temperature.

Permafrost thaw in regions with relatively high organic soil matter content is of concern because of how much carbon can potentially be released into the atmosphere, so we assess the variability in future ALTMAX and TSOI in four sub-regions across the permafrost area. Each region, outlined on the map in Figure 1, has observed high organic soil matter content: three of the four regions (Alaska, Siberia, and the Tibetan Plateau) have high concentrations of observed Yedoma permafrost (Strauss et al., 2021) and the fourth (Canada) is extensively covered by peatlands (Tarnocai et al., 2011; Wells et al., 2010). Since all permafrost soils can release stored carbon, we also look at variability across the entire boreal permafrost region.

Finally, we consider the formation of talik, or perennially unfrozen soil within or above permafrost, to be a quantifiable precursor to a potential permafrost tipping point. Following the definition used by Parazoo et al. (2018) for talik in an Earth system model, the first year of talik formation is the first year when the monthly mean temperature of any subsurface layer in a permafrost grid cell exceeds −0.5°C and remains above −0.5°C for at least 24 consecutive months. The cutoff of −0.5°C is similar to the −0.3°C temperature cutoff used by Farquharson et al. (2022) for assessing talik formation in a high-resolution numerical model (Jafarov et al., 2012).

2.3. Logistic Regression Model

To determine when the influence of SAI on permafrost-related fields might be detectable, we trained two logistic regression models (Box et al., 2015) to predict the probability that a map of ALT or TSOI is from the ARISE-SAI-1.5 or SSP2-4.5 simulation. The maps are restricted to the boreal permafrost region from 50 to 84°N, which are

flattened into arrays of 10,656 units, or 37 latitude by 288 longitude points. The arrays are normalized to a mean of 0 and a standard deviation of 1 across all grid points. For each variable, the model receives these flattened and normalized arrays as input vectors. The output layer of the logistic regression models produce values that, when passed through the sigmoid activation function, can be interpreted as the probability that the map comes from either the ARISE-SAI-1.5 or SSP2-4.5 simulation. More information about the models' architecture is in Tables S1 and S2 of Supporting Information S1. Each model is trained on seven ensemble members, validated on two, and tested on one. The models are trained on the full 35-year experiment (2035–2069).

To better understand which permafrost regions are most helpful for the logistic regression models to make their predictions, we also perform feature contribution analysis. Feature contribution is a method to improve interpretability of the logistic regression models by identifying which regions contributed to the prediction that a map came from either the ARISE-SAI-1.5 or SSP2-4.5 simulations. Contribution maps are created by multiplying the model weights by the annual mean input values for either ALT or TSOI at every grid point. Positive (negative) contributions are regions that drive the model toward predicting a map is from the ARISE-SAI-1.5 simulations and negative contributions are regions that drive the model toward predicting a map is from SSP2-4.5. The more positive or negative the contribution of a particular point or region, the more "important" that point or region is for driving the logistic regression model prediction toward either the ARISE-SAI-1.5 or SSP2-4.5 simulations.

3. Results

3.1. Natural Variability in Permafrost Fields

We begin by evaluating projected natural and regional variability in the active layer and in soil temperature. Figure 2 shows time series of the annual maximum active layer depth (ALTMAX) in the four selected regions (Figures 2a–2d) and across the entire permafrost region (Figure 2e) in the SSP2-4.5 (red dashed lines) and ARISE-SAI-1.5 (blue solid lines) simulations. We include a map of the EM ALTMAX in 2034 from the SSP2-4.5 simulation as reference for the spatial pattern of ALTMAX in the year before SAI deployment (center map, Figure 2). There is a lot of regional variability between all five panels (note the panel scale differences), with the deepest ALTMAX in both simulations in Canada peatland (Figure 2a) and the shallowest in Siberia Yedoma (Figure 2d). The EMs of the two simulations (thick lines) diverge soon after SAI deployment in 2035, with the SSP2-4.5 EM ALTMAX getting deeper in response to increasing surface temperatures and the ARISE-SAI-1.5 EM either stabilizing or getting shallower in response to stabilizing surface temperatures. By 2045, the EM ALTMAX in SSP2-4.5 is 6–61 cm deeper than in ARISE-SAI-1.5 in all five regions, and 21–201 cm deeper in SSP2-4.5 than in ARISE-SAI-1.5 by the end of the simulations in 2069.

The individual ALTMAX ensemble members (thin lines) continue to overlap between the two simulations for several years after SAI deployment. Indeed, only in Siberia Yedoma (Figure 2d) and the entire permafrost region (Figure 2e) do all the ARISE-SAI-1.5 realizations fully diverge from all the SSP2-4.5 realizations by 2069. The overlap between ensemble members indicates that internal variability may mask the forced response of permafrost to SAI and make it hard to distinguish one climate realization from another when it comes to an SAI versus non-SAI world. Additionally, SAI may not be perceived as "successful" in some ensemble members where ALTMAX exhibits an increasing trend immediately after SAI (see Figure 2a), even if ALTMAX eventually stabilizes and begins to decrease.

ALTMAX trends pre- and post-SAI deployment are highly variable by region and by ensemble member. In the decade preceding SAI deployment (2025–2034; Figure 3a) the ALTMAX trend in ensemble member #3 is positive across Canada but almost entirely negative across Siberia, while in ensemble member #10 the trends are positive in far eastern and western Russia. Regionally the active layer can get deeper or shallower (trends for all ensemble members are in Figure S1 in Supporting Information S1), despite a generally positive ALTMAX trend in the forced response (see the EM), especially along the southern margin of the permafrost region.

ALTMAX trends are also highly variable in the decade following SAI deployment (2035–2044; Figure 3b). The active layer gets deeper in far eastern and western Russia in ensemble member #3, but otherwise exhibits similar ALTMAX trends as the previous decade (Figure 3a). In contrast to ensemble member #3, ensemble member #10

10.1029/2023EF004191

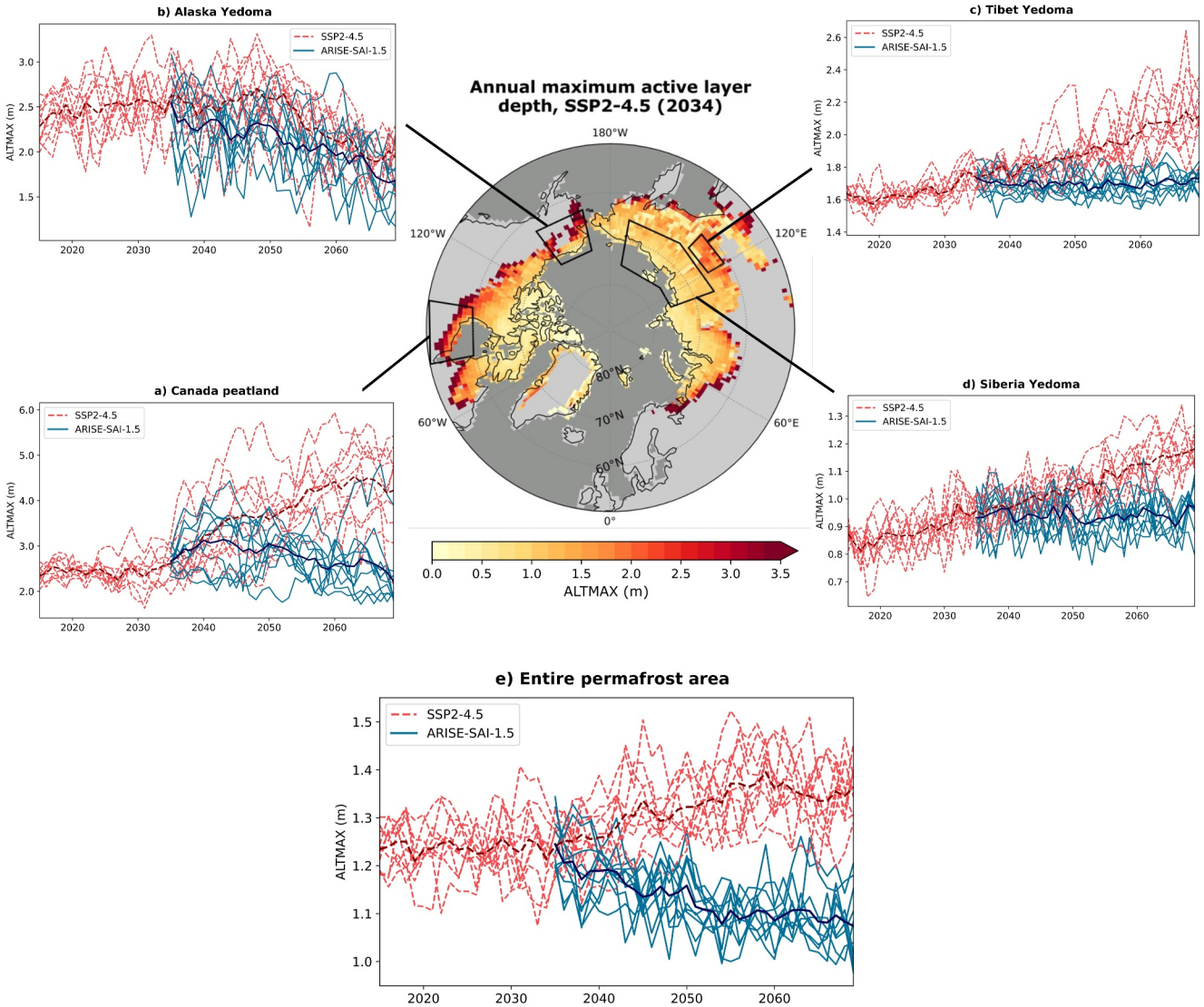

Figure 2. Time series of annual maximum active layer depth (ALTMAX) in SSP2-4.5 (red dashed lines) and ARISE-SAI-1.5 (blue solid lines) within (a) Canada peatland, (b) Alaska Yedoma, (c) Siberia Yedoma, (d) Tibet Yedoma, and (e) the entire permafrost region. The regions in (a–d) are identified in Figure 1. Thin lines are individual ensemble members; thick lines are the ensemble means (EMs). The central map is the EM annual maximum active layer depth in SSP2-4.5 in 2034.

shows decreasing ALTMAX trends across the entire permafrost region, with the largest trends in eastern Canada and near the Hudson Bay. While not all ensemble members have differing trends pre- and post-deployment (Figures S1 and S2 in Supporting Information S1), ensemble members #3 and #10 are examples of how natural variability could lead to SAI being perceived as "successful" at preventing permafrost thaw (i.e., a positive ALTMAX trend into a negative trend) or as "failing" to prevent permafrost thaw (i.e., a negative or neutral ALTMAX trend into a positive trend). Compared to trends in individual ensemble members, the EM ALTMAX trends are relatively small, except for along the margins of the permafrost region.

As for ALTMAX (Figure 2), the annual mean time series of the permafrost temperature (TSOI) in the four regions with high organic soil matter content (Figures 4a–4d) and across the entire permafrost region (Figure 4e) exhibit large regional and natural variability. As expected, the warmest permafrost temperatures are at the lowest latitude of the permafrost extent, and get colder with increasing latitude (center map, Figure 4). While the EM annual mean TSOI (thick lines) increases in all regions from 2015 to 2069 in SSP2-4.5 (red dashed lines), permafrost reaches the warmest temperatures in Canada peatland (Figure 4a). TSOI either stabilizes or decreases in all regions in ARISE-SAI-1.5 (blue solid lines), but there is a large range in projected temperature. In a single year,

10.1029/2023EF004191

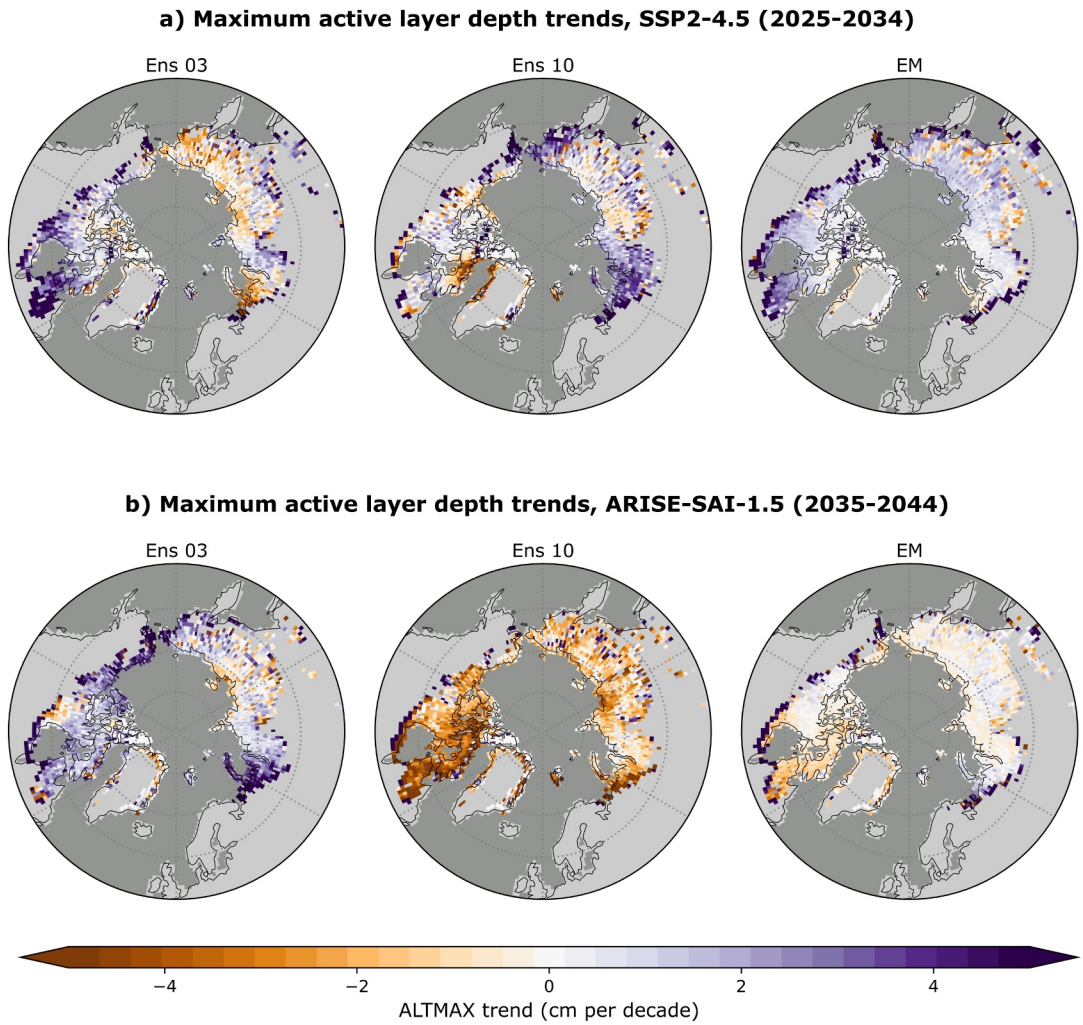

Figure 3. Decadal trends in maximum active layer depth (ALTMAX) in ensemble members #3 and #10 and the 10-member ensemble mean (EM) in (a) SSP2-4.5 from 2025 to 2034, or the decade immediately preceding stratospheric aerosol injection (SAI) deployment and (b) ARISE-SAI-1.5 from 2035 to 2044, or the decade immediately following SAI deployment. Trends are calculated using least squares regression. Purple (orange) means the active layer gets deeper (shallower).

TSOI can span several degrees between individual ensemble members. Similar to ALTMAX, the TSOI time series in ARISE-SAI-1.5 and SSP2-4.5 only fully diverge in Siberia Yedoma (Figure 4d) and when averaged over the entire permafrost region (Figure 4e).

Given the large spread in TSOI between ensemble members (Figure 4), it is perhaps unsurprising that there is also a large spread in pre- and post-SAI deployment decadal temperature trends (Figure 5; Figures S3 and S4 in Supporting Information S1). Most ensemble members, including #3 and #10, show warming trends of >0.3°C decade^{-1} in the decade leading up to SAI deployment (Figure 5a; Figure S3 in Supporting Information S1), but temperature trends are highly regionally variable. Most of Canada strongly warms in ensemble member #3 from 2025 to 2034 (Figure 5a), and continues to warm in 2035–2044 post-SAI deployment (Figure 5b). In ensemble member #10, however, temperature trends go from warming to a strong cooling trend across the entire permafrost region, indicating that SAI may be perceived as "successful" at preventing the permafrost soil temperature from increasing. Along with variability in 2035–2044 temperature trends between ensemble members (Figure S4 in Supporting Information S1), there is a lot of spatial heterogeneity in most ensemble members' TSOI trends, resulting in a near-zero EM trend across the entire permafrost region. As a result, interpreting SAI's influence on permafrost temperature simply from the EM would lead to the conclusion that SAI has little effect on temperature, a conclusion that is not supported by any single ensemble member.

10.1029/2023EF004191

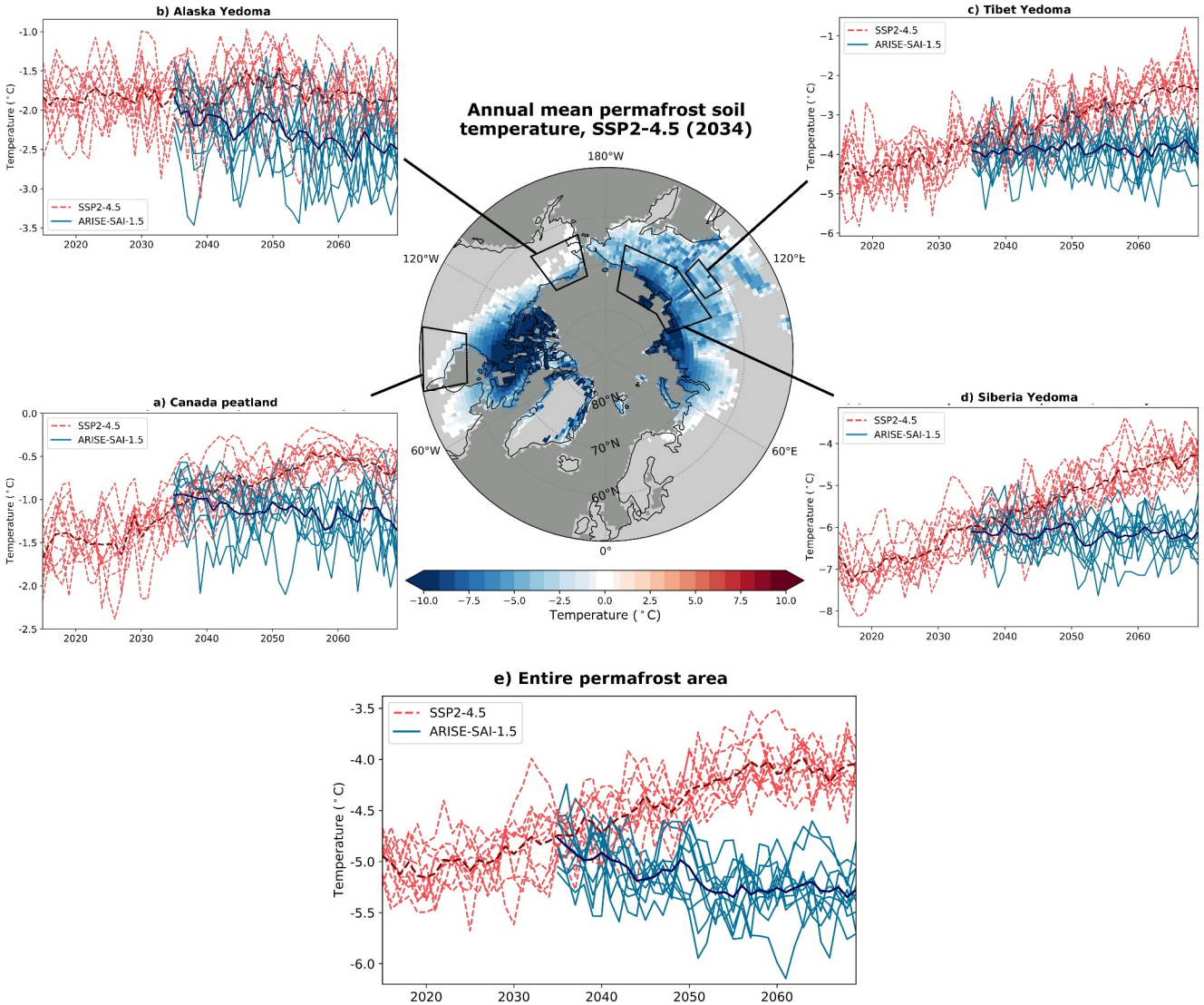

Figure 4. As in Figure 2 except for the annual mean permafrost soil temperature (TSOI).

3.2. Detecting Permafrost Response to SAI

Given the large spread in permafrost fields driven by internal climate variability in both the SSP2-4.5 and ARISE-SAI-1.5 simulations, we next move to trying to quantify how long it might take to tell if or when SAI is influencing permafrost. To do this, we use logistic regression models that learn the patterns of active layer depth and soil-to-bedrock temperature that occur in an SAI and non-SAI world. How long does it take the models to confidently predict which simulation a map of annual mean ALT or TSOI comes from? For ALT, the model correctly predicts which maps belong to which simulation starting in 2060 (Figure 6a). That is, it takes almost 30 years of SAI deployment for the model to be confident and accurate in its prediction that a map of annual mean active layer depth comes from an SAI or non-SAI world. Model confidence is nearly 100% for the SSP2-4.5 predictions (red line) by 2050, but only reaches 100% confidence for the ARISE-SAI-1.5 predictions (blue line) at the end of the simulations. It takes fewer years of SAI deployment for the model to identify the correct simulations for maps of annual mean TSOI (Figure 6b). The model achieves perfect accuracy for both simulations starting in 2051, and reaches near-100% confidence in its predictions for both the SSP2-4.5 and ARISE-SAI-1.5 maps in 2066. These results are robust to which members are used for training and validation.

10.1029/2023EF004191

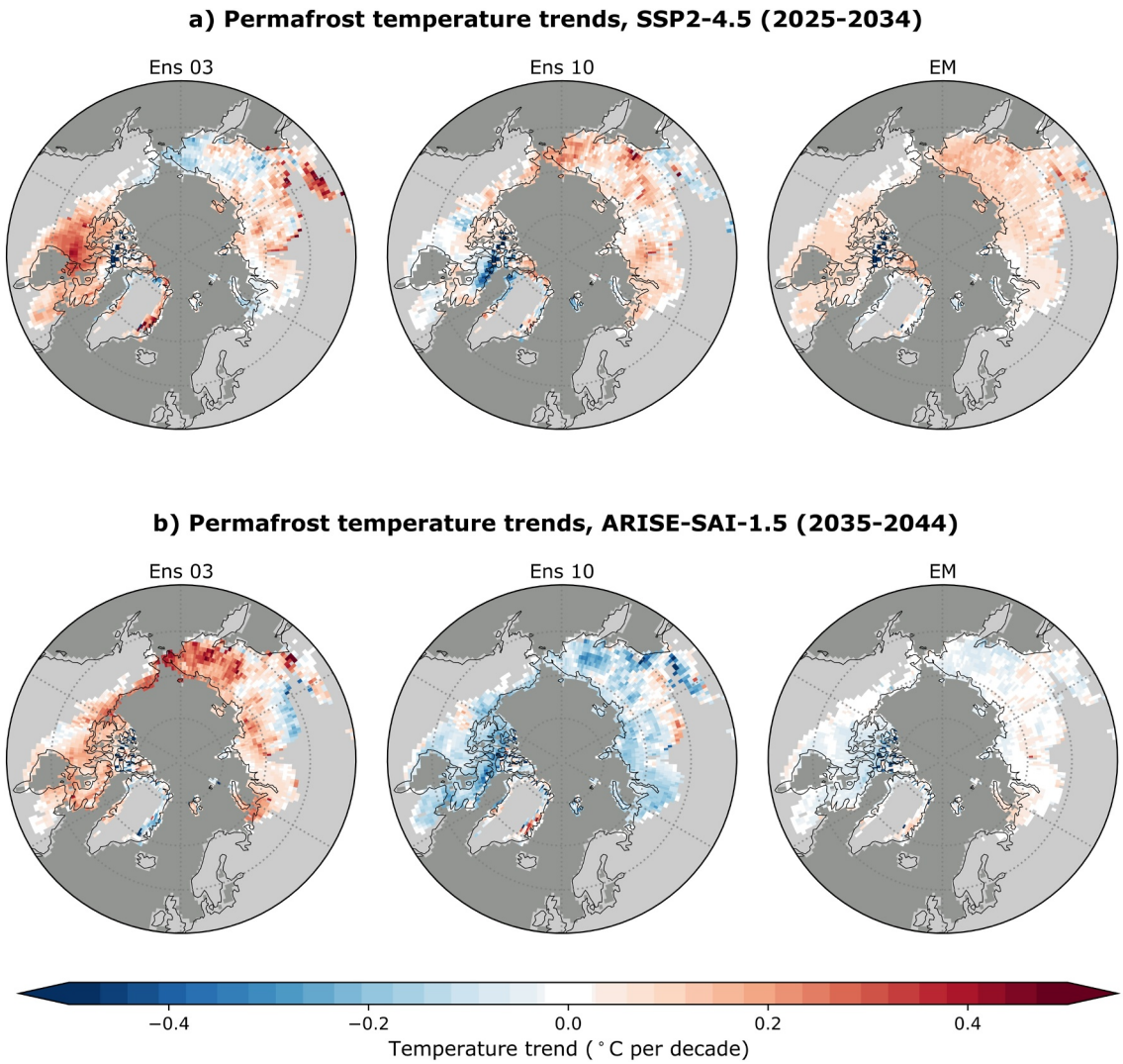

Figure 5. As in Figure 3 except for the annual mean permafrost soil temperature (TSOI).

Certain regional patterns of ALT and TSOI help the logistic regression models achieve perfect accuracy in their predictions, and we use contribution maps to identify these patterns. For ALT predictions, the areas that provide the largest contribution are found along the lowest latitude of the permafrost region (Figure 7a), and the rest of the permafrost region has a negligible contribution to the model prediction. The largest contributions are positive, meaning that the ALT information along the permafrost margins contributed to the logistic regression model predicting that the map came from the ARISE-SAI-1.5 simulation. The margins are where the active layer is deepest (Figure 2), and where it is rapidly deepening in SSP2-4.5. The margins are also where ALT slowly stabilizes and stops getting deeper in ARISE-SAI-1.5 (Figure 2). SAI eventually prevents the active layer from getting deeper, but this stabilization process takes many years, hence why the detection of SAI's influence on ALT also takes many years.

Temperature contributions to the logistic regression model predictions are far more heterogeneous than ALT contributions and come from the entire permafrost region (Figure 7b). The largest positive contributions, or the regions that make a map more likely to be from the ARISE-SAI-1.5 simulations, are also in the same regions with positive ALT contributions (Figure 7a). Regions with a deeper active layer have warmer soil because it means that more of the soil is thawed. Regions that push the prediction toward the SSP2-4.5 simulations (largest negative contributions) are concentrated near the Tibet Yedoma region. Most of Canada, except for grid cells along the

10.1029/2023EF004191

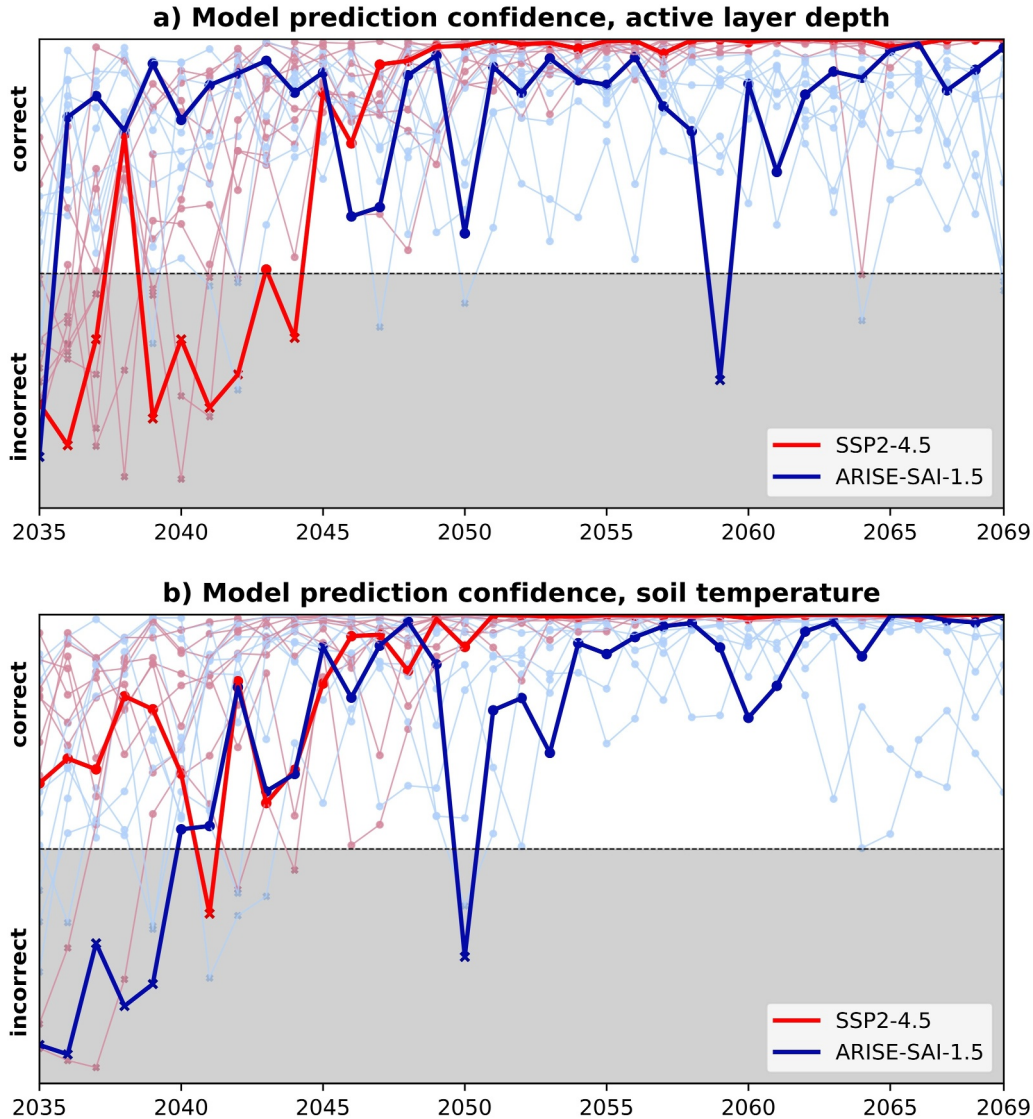

Figure 6. Logistic regression model confidence for the single testing member (bold line) and the training and validation members (thin lines) of the SSP2-4.5 (red) and ARISE-SAI-1.5 (blue) simulations for annual mean maps of (a) active layer depth and (b) soil temperature down to the bedrock in grid cells with permafrost.

southern margin of permafrost, also contributes to the logistic regression model predicting that a map of TSOI comes from SSP2-4.5.

3.3. Likelihood of Talik Formation Affected by Natural Variability

Since there is a large range of outcomes for active layer thickness and soil temperature in SAI and non-SAI worlds, there may also be a large range of outcomes for a key climatic concern from permafrost thaw - namely, the formation of talik that could lead to widespread, accelerated, and irreversible thaw and carbon release. The difference in the timing of talik formation, or the first year that permafrost reaches a potential tipping condition, between the SSP2-4.5 and ARISE-SAI-1.5 simulations is shown for each ensemble member and the EM in Figure 8. The dark blue and cyan cells are where talik formation has either been delayed or completely prevented in ARISE-SAI-1.5 compared to the corresponding SSP2-4.5 member. Red and yellow cells are where talik has either formed earlier under SAI than in SSP2-4.5, or, in rare cases, has formed under SAI but does not form in SSP2-4.5 by 2069. Black cells are where permafrost has degraded enough under SSP2-4.5 forcing conditions that unfrozen ground already exists within or above the permafrost by 2035. Most of the Alaska

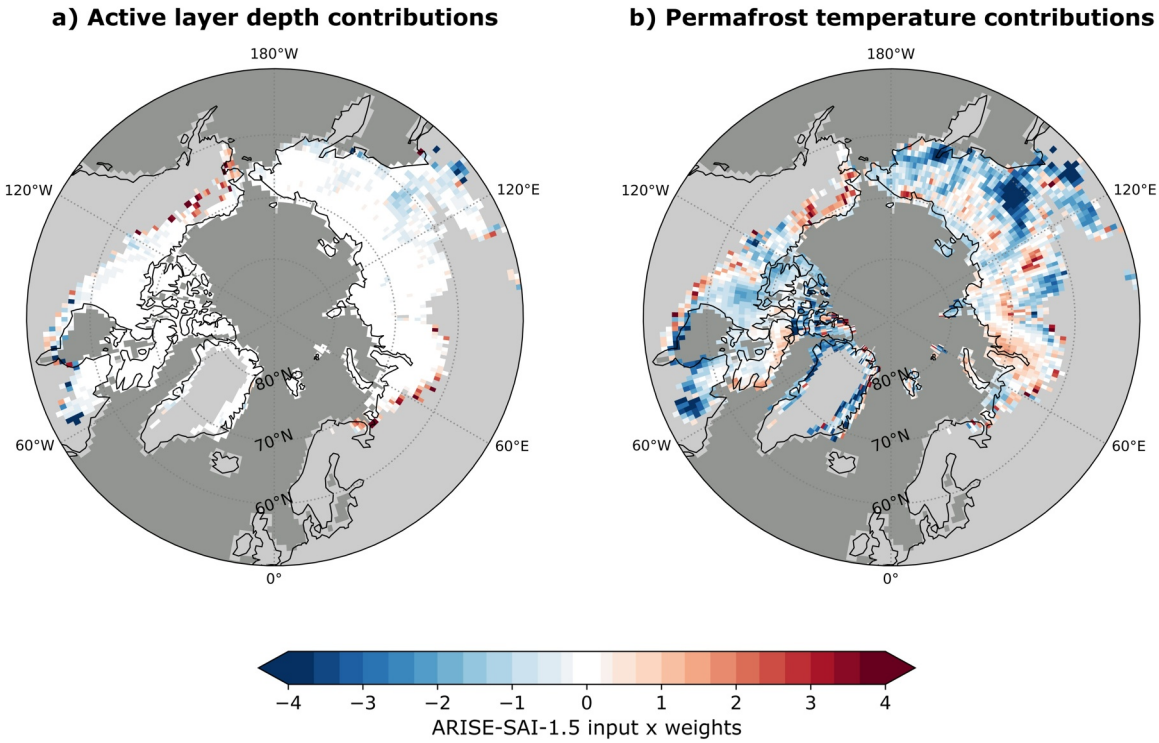

Figure 7. Contribution maps (input × weights) for the ARISE-SAI-1.5 testing ensemble member averaged over 2035–2069 for (a) active layer depth and (b) permafrost temperature logistic regression model predictions.

Yedoma region is degraded permafrost, except for the Alaska North Slope, and therefore SAI cannot prevent talik formation here under the ARISE-SAI-1.5 scenario. Outside of the highly degraded permafrost, there are some other regions where SAI is not successful in delaying talik formation. In 50% of ensemble members, talik forms earlier in some cells within the Canada peatland region under SAI (pink and red cells). Of all the non-degraded permafrost regions, Canada peatland is where SAI most often fails to delay or prevent talik formation. Soil temperatures are warmer in Canada peatland than in the Tibet and Siberia Yedoma regions (Figure 4), and taliks form as a result of thermal or hydrologic anomalies. Once a talik forms it is very difficult to refreeze that ground (Devoie et al., 2019). Outside of Canada peatland and the degraded permafrost regions, SAI does prevent or delay most talik formation in all ensemble members and in the EM (note the widespread cyan cells).

Regional and natural variability in permafrost lead to a range of outcomes in projected talik formation. Figure 9 shows the probability that talik is prevented in the ARISE-SAI-1.5 ensemble members compared to the corresponding SSP2-4.5 ensemble members. The probabilities are calculated only for the ensemble members that formed talik in SSP2-4.5. For example, if eight members formed talik in SSP2-4.5 and six of those members did not form talik in ARISE-SAI-1.5, the probability of talik prevention under SAI is 75%. The blue crossed hatching in Figure 9 is where fewer than five members formed talik in SSP2-4.5, and the green dashed hatching is where all 10 members formed talik in SSP2-4.5. Some regions are clearly more susceptible to talik formation even under SAI, due to the influence of natural variability (darker colored cells in Figure 9), while some regions appear to be robustly resistant to talik formation - that is, ARISE-SAI-1.5 completely prevents talik relative to SSP2-4.5 (bright yellow cells in Figure 9), not just delays it. As shown in Figure 8, there is strong agreement between all ensemble members that talik already exists along the southern permafrost margin by the time SAI is deployed in 2035 (green hatching over black cells in Figure 9), and there is a 0% probability that SAI can prevent this talik from forming. Outside of the degraded permafrost cells where talik already exists by 2035, talik formation is most often robustly (>5 ensemble member agreement) prevented in north-central Canada, and least often robustly prevented in the Canada peatland area and north-east Canada. Importantly, talik formation is prevented under the ARISE-SAI-1.5 scenario in at least one ensemble member in every grid cell where talik did not already exist by 2035.

10.1029/2023EF004191

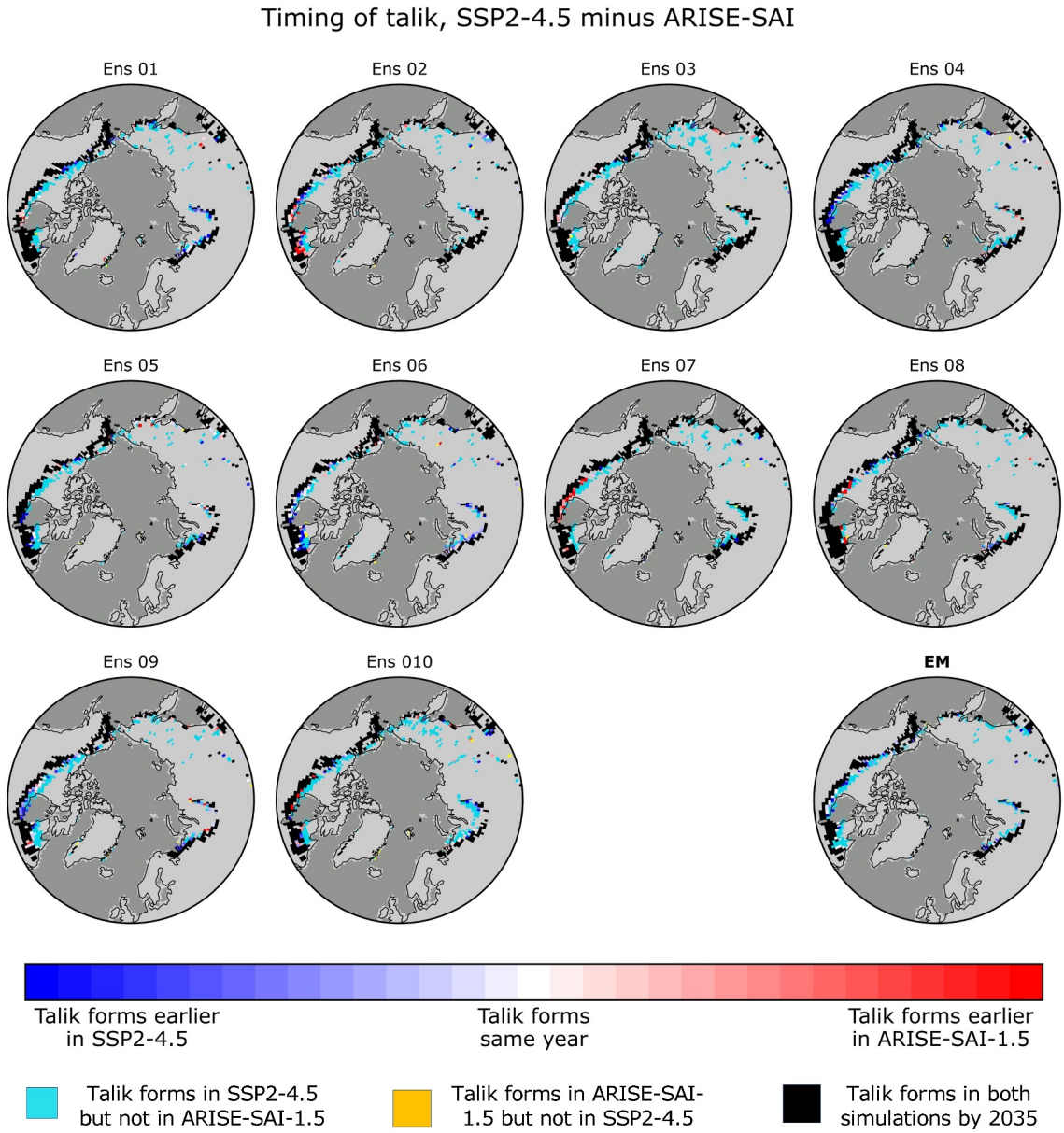

Figure 8. Difference in the timing of projected talik formation in each ensemble member, SSP2-4.5 minus ARISE-SAI-1.5. Cyan cells are where talik forms in an SSP2-4.5 ensemble member by 2069 but never forms in the corresponding ARISE-SAI-1.5 ensemble member. Yellow cells are where talik forms in an ARISE-SAI-1.5 ensemble member by 2069 but never forms in the corresponding SSP2-4.5 ensemble member. Black cells are where talik exists by 2035 in the ensemble member for both simulations. The final map is the difference in the timing of projected talik formation in the 10-member ensemble mean.

4. Discussion and Conclusions

Overall our results show that natural climate variability leads to a range of projected outcomes for ALTMAX and TSOI with and without SAI. In four regions with high organic soil matter content, natural variability in both ALTMAX and TSOI makes it difficult to distinguish between individual ensemble members in the ARISE-SAI-1.5 and SSP2-4.5 simulations for several years after SAI deployment. The overlap between the simulations means that it may take decades of aerosol deployment before SAI has a noticeable effect on permafrost Yedoma and peatland. These results support previous work that SAI could prevent permafrost thaw in the forced response (Chen et al., 2020, Chen et al., 2023; H. Lee et al., 2019; W. Lee et al., 2023; Liu et al., 2023; Morrison et al., 2024), though to our knowledge this is the first work to assess the extent to which natural variability may mask the forced permafrost response to SAI.

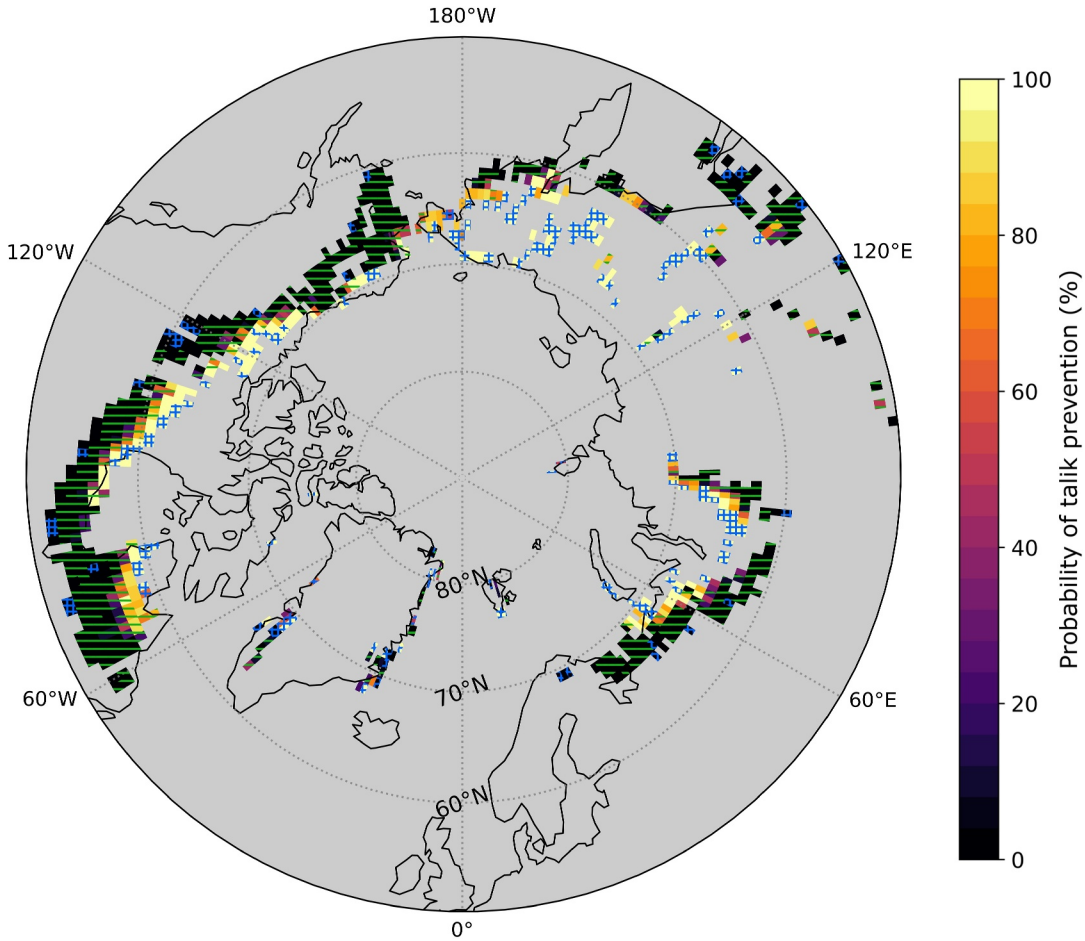

Figure 9. Probability that talik formation is prevented in ARISE-SAI-1.5 ensemble members compared to corresponding SSP2-4.5 ensemble members. Probabilities are calculated for the number of ensemble members where talik formed in the SSP2-4.5 simulation. Blue crossed hatching means that fewer than five ensemble members formed talik in that grid cell in SSP2-4.5. Green dashed hatching means that all 10 ensemble members formed talik in that grid cell in SSP2-4.5.

There is also a range in the projected timing of talik formation even under SAI, but this is highly regionally dependent. All ensemble members are in agreement that the southern margin of permafrost already contains talik by 2035 (green hatching over the black cells in Figure 9), and therefore talik forms along the southern margin regardless of any SAI influence. As a result, the southernmost permafrost is very likely to be lost no matter what impact SAI has on the rest of the permafrost region under ARISE-SAI-1.5. Most of the Alaska Yedoma region already contains talik by 2035 (Figure 9). This pre-SAI talik may explain why ALTMAX appears to stabilize and become shallower over time in the Alaska Yedoma region (Figure 2b): the deepest ALTMAX is over the warmest and most degraded permafrost and once the warm permafrost thaws, the remaining permafrost is more stable and exists under a shallower active layer. All members are also in agreement that SAI as deployed by ARISE-SAI-1.5 prevents the majority of pan-Arctic talik formation outside of the southern margin.

Why is the SAI influence detectable earlier on soil temperature than on active layer depth? TSOI responds faster to increasing surface temperatures in SSP2-4.5 than the active layer does. The active layer thickness cannot increase until the soil temperature in a deeper layer exceeds 0°C, so TSOI changes faster than ALT does. Since permafrost temperature remains below freezing, but does get warmer in SSP2-4.5 (Figure 2), the soil is not thawing quickly enough to increase the active layer depth. Permafrost temperature changes rapidly enough in the SSP2-4.5 simulations to distinguish a map of TSOI between the two simulations earlier than a map of ALT. TSOI is also changing everywhere, which is why contributions to the TSOI predictions come from the entire permafrost region (Figure 7b). Once permafrost thaws and the active layer deepens, it is very difficult to refreeze permafrost and reduce the active layer depth (Devoie et al., 2019). This is particularly difficult if talik has formed between the

permafrost and base of the active layer (Connon et al., 2018). Once the permafrost is completely thawed, there is no more ALT in the SSP2-4.5 simulations. The logistic regression model uses the pattern of ALT loss to differentiate between the ARISE-SAI-1.5 and SSP2-4.5 simulations, which is why the ALT prediction contributions are only from the permafrost margins (Figure 7a): if a map of ALT has an active layer on the southern permafrost margin, then it belongs to the ARISE-SAI-1.5 simulation.

Although our results come from a single idealized SAI scenario that is simulated by one Earth system model, models are the best available tools for assessing possible impacts of SAI. Models are the only way to study climate projections, and using ensembles of different climate realizations also gives us insight into how natural variability may affect climate outcomes. Different processes can be easier or harder to simulate in models, however. Permafrost is difficult to simulate because it is affected by subgrid-scale processes that are not yet represented in the current generation of climate models. We do not specifically identify subaerial talik (formed below a lake), which is a common location for talik to be found in observations (Devoie et al., 2019), and therefore may be underestimating the extent of talik formation in CESM2. It is important to note that talik formation is a precursor to widespread permafrost thaw in observations (Connon et al., 2018; Devoie et al., 2019), but the 35-year simulation may be too short to determine if a permafrost tipping point actually occurs. Permafrost outcomes may be very different under an SAI scenario that reduces global mean surface temperature instead of stabilizing it at 1.5°C, such as those considered by MacMartin et al. (2022).

Our results indicate that SAI as simulated by the ARISE-SAI-1.5 scenario generally preserves permafrost and stabilizes both ALTMAX and TSOI at near-2035 levels, though it may take one to three decades of SAI deployment to robustly detect its influence on both permafrost fields. Natural variability may lead to a climate future where ALTMAX or TSOI increase in the decade following SAI deployment, contrary to the forced response. Interpreting the effects of SAI on permafrost only from the forced response (i.e., the EMs) may lead to a possibly erroneous conclusion that SAI could quickly preserve permafrost and prevent talik formation. Assessing the forced response is critical for improving our understanding of how SAI may affect different aspects of the climate system, but there is no guarantee that our future climate will resemble the outcome of the EM. This study highlights the importance of accounting for natural variability when assessing the potential impact of SAI on the climate system, especially if SAI is deployed in an effort to prevent climate tipping points.

Conflict of Interest

The authors declare no conflicts of interest relevant to this study.

Data Availability Statement

The code for this analysis is available from Morrison (2024). All unprocessed monthly mean CESM2 ARISE-SAI-1.5 and SSP2-4.5 data that support this study are publicly available from Richter (2022) and Mills et al. (2022).

Acknowledgments
This work was supported by Defense Advanced Research Projects Agency Grant HR00112290071. The views expressed here do not necessarily reflect the positions of the U.S. government. We would like to acknowledge high-performance computing support from Cheyenne (https://doi.org/10.5065/D6RX99HX) provided by NCAR's Computational and Information Systems Laboratory, sponsored by the National Science Foundation. A.L.M. and J.W.H. were also supported by the LAD climate group. We would like to thank two anonymous reviewers for their constructive comments that improved the manuscript, and D. Lawrence for his helpful suggestions and comments on CLM5, talik, and permafrost.

References

Armstrong McKay, D., Staal, A., Abrams, J., Winkelmann, R., Sakschewski, B., Loriani, S., et al. (2022). Exceeding 1.5°C global warming could trigger multiple tipping points. *Science*, *377*(6611), eabn7950. https://doi.org/10.1126/science.abn7950

Barnes, E., Hurrell, J., & Sun, L. (2022). Detecting changes in global extremes under the GLENS-SAI climate intervention strategy. *Geophysical Research Letters*, *49*(20), e2022GL100198. https://doi.org/10.1029/2022GL100198

Box, G., Jenkins, G., Reinsel, G., & Ljung, G. (2015). *Time series analysis: Forecasting and control* (5th ed.). Wiley.

Burke, E. J., Zhang, Y., & Krinner, G. (2020). Evaluating permafrost physics in the Coupled Model Intercomparison Project 6 (CMIP6) models and their sensitivity to climate change. *The Cryosphere*, *14*(9), 3155–3174. https://doi.org/10.5194/tc-14-3155-2020

Chen, Y., Ji, D., Zhang, Q., Moore, J. C., Boucher, O., Jones, A., et al. (2023). Northern-high-latitude permafrost and terrestrial carbon response to two solar geoengineering scenarios. *Earth System Dynamics*, *14*(1), 55–79. https://doi.org/10.5194/esd-14-55-2023

Chen, Y., Liu, A., & Moore, J. (2020). Mitigation of arctic permafrost carbon loss through stratospheric aerosol geoengineering. *Nature Communications*, *11*(2430), 2430. https://doi.org/10.1038/s41467-020-16357-8

Connon, R. F., Devoie, E. G., Hayashi, M., Veness, T., & Quinton, Q. (2018). The influence of shallow taliks on permafrost thaw and active layer dynamics in subarctic Canada. *Journal of Geophysical Research: Earth Surface*, *123*(2), 281–297. https://doi.org/10.1002/2017JF004469

Dagon, K., & Schrag, D. P. (2017). Regional climate variability under model simulations of solar geoengineering. *Journal of Geophysical Research: Atmospheres*, *122*(22), 12106–12121. https://doi.org/10.1002/2017JD027110

Danabasoglu, G., Lamarque, J.-F., Bacmeister, J., Bailey, D., DuVivier, A., Edwards, J., et al. (2020). The community earth system model version 2 (CESM2). *Journal of Advances in Modeling Earth Systems*, *12*(2), e2019MS001916. https://doi.org/10.1029/2019MS001916

Deser, C., Phillips, A. S., Alexander, M. A., & Smoliak, B. V. (2014). Projecting North American climate over the next 50 years: Uncertainty due to internal variability. *Journal of Climate*, *27*(6), 2271–2296. https://doi.org/10.1175/JCLI-D-13-00451.1

Devoie, E. G., Craig, J. R., Connon, R. F., & Quinton, W. L. (2019). Taliks: A tipping point in discontinuous permafrost degradation in peatlands. *Water Resources Research*, *55*(11), 9839–9857. https://doi.org/10.1029/2018WR024488

Farquharson, L. M., Romanovsky, V. E., Kholodov, A., & Nicolsky, D. (2022). Sub-aerial talik formation observed across the discontinuous permafrost zone of Alaska. *Nature Geoscience*, *15*(6), 475–481. https://doi.org/10.1038/s41561-022-00952-z

Gettelman, A., Mills, M., Kinnison, D., Garcia, R., Smith, A., Marsh, D., et al. (2019). The whole atmosphere community climate model version 6 (WACCM6). *Journal of Geophysical Research: Atmospheres*, *124*(23), 12380–12403. https://doi.org/10.1029/2019JD030943

Gulev, S. K., Thorne, P. W., Ahn, J., Dentener, F. J., Domingues, C. M., Gerland, S., et al. (2021). Changing state of the climate system. In V. Masson-Delmotte, P. Zhai, A. Pirani, S. L. Connors, C. Pean, S. Berger, et al. (Eds.), *Climate change 2021: The physical science basis. Contribution of Working Group I to the Sixth Assessment Report of the Intergovernmental Panel on Climate Change*. Cambridge University Press.

Hueholt, D. M., Barnes, E. A., Hurrell, J. W., Richter, J. H., & Sun, L. (2023). Assessing outcomes in stratospheric aerosol injection scenarios shortly after deployment. *Earth's Future*, *11*(5), e2023EF003488. https://doi.org/10.1029/2023EF0034881

Hugelius, G., Loisel, J., Chadburn, S., Jackson, R. B., Jones, M., MacDonald, G., et al. (2020). Large stocks of peatland carbon and nitrogen are vulnerable to permafrost thaw. *Proceedings of the National Academy of Sciences*, *117*(34), 20438–20446. https://doi.org/10.1073/pnas.1916387117

Hugelius, G., Strauss, J., Zubrzycki, S., Harde, J. W., Schuur, E. A. G., Ping, C.-L., et al. (2014). Estimated stocks of circumpolar permafrost carbon with quantified uncertainty ranges and identified data gaps. *Biogeosciences*, *11*(23), 6573–6593. https://doi.org/10.5194/bg-11-6573-2014

Jafarov, E. E., Marchenko, S. S., & Romanovsky, V. E. (2012). Numerical modeling of permafrost dynamics in Alaska using a high spatial resolution dataset. *The Cryosphere*, *6*(3), 613–624. https://doi.org/10.5194/tc-6-613-2012

Jones, A., Hawcroft, M., Haywood, J., Jones, A., Guo, X., & Moore, J. (2018). Regional climate impacts of stabilizing global warming at 1.5 K using solar geoengineering. *Earth's Future*, *6*(2), 230–251. https://doi.org/10.1002/2017ef000720

Keys, P. W., Barnes, E. A., Diffenbaugh, N. S., Hurrell, J. W., & Bell, C. M. (2022). Potential for perceived failure of stratospheric aerosol injection deployment. *Proceedings of the National Academy of Sciences*, *119*(40), e2210036119. https://doi.org/10.1073/pnas.2210036119

Kravitz, B., MacMartin, D., Tilmes, S., Richter, J., Mills, M., Cheng, W., et al. (2019). Comparing surface and stratospheric impacts of geoengineering with different SO_2 injection strategies. *Journal of Geophysical Research: Atmospheres*, *124*(14), 7900–7918. https://doi.org/10.1029/2019jd030329

Kravitz, B., MacMartin, D. G., Mills, M. J., Richter, J. H., Tilmes, S., Lamarque, J.-F., et al. (2017). First simulations of designing stratospheric sulfate aerosol geoengineering to meet multiple simultaneous climate objectives. *Journal of Geophysical Research: Atmospheres*, *122*(23), 12616–12634. https://doi.org/10.1002/2017jd026874

Kravitz, B., Robock, A., Boucher, O., Schmidt, H., Taylor, K., Stenchikov, G., & Schulz, M. (2011). The geoengineering model intercomparison project (GeoMIP). *Journal of Geophysical Research*, *12*(2), 162–167. https://doi.org/10.1002/asl.316

Labe, Z. M., Barnes, E. A., & Hurrell, J. W. (2023). Identifying the regional emergence of climate patterns in the ARISE-SAI-1.5 simulations. *Environmental Research Letters*, *18*(4), 044031. https://doi.org/10.1088/1748-9326/acc81a

Lawrence, D., Fisher, R., Koven, C., Oleson, K., Swenson, S., Bonan, G., et al. (2019). The community land model version 5: Description of new features, benchmarking, and impact of forcing uncertainty. *Journal of Advances in Modeling Earth Systems*, *11*(12), 4245–4287. https://doi.org/10.1029/2018ms001583

Lawrence, D., Fisher, R., Koven, C., Oleson, K., Swenson, S., Vertenstein, M., et al. (2018). *Technical description of version 5.0 of the community land model (CLM)* [Report]. National Center for Atmospheric Research. Retrieved from https://www2.cesm.ucar.edu/models/cesm2/land/CLM50_Tech_Note.pdf

Lee, H., Altug, E., Tjiputra, J., Muri, H., Chadburn, S. E., Lawrence, D. M., & Schwinger, J. (2019). The response of permafrost and high-latitude ecosystems under large-scale stratospheric aerosol injection and its termination. *Earth's Future*, *7*(6), 605–614. https://doi.org/10.1029/2018EF001146

Lee, W., MacMartin, D. G., Visioni, D., Kravitz, B., Chen, Y., Moore, J. C., et al. (2023). High-latitude stratospheric aerosol injection to preserve the Arctic. *Earth's Future*, *11*(1), e2022EF003052. https://doi.org/10.1029/2022EF003052

Lenton, T. (2012). Arctic climate tipping points. *Ambio*, *41*(1), 10–22. https://doi.org/10.1007/s13280-011-0221-x

Liu, A., Moore, J. C., & Chen, Y. (2023). PInc-PanTher estimates of Arctic permafrost soil carbon under the GeoMIP G6solar and G6sulfur experiments. *Earth System Dynamics*, *14*(1), 39–53. https://doi.org/10.5194/esd-14-39-2023

MacMartin, D. G., Kravitz, B., Keith, D. W., & Jarvis, A. (2014). Dynamics of the coupled human–climate system resulting from closed-loop control of solar geoengineering. *Climate Dynamics*, *43*(1–2), 243–258. https://doi.org/10.1007/s00382-013-1822-9

MacMartin, D. G., Visioni, D., Kravitz, B., Richter, J. H., Felgenhauer, T., Lee, W. R., et al. (2022). Scenarios for modeling solar radiation modification. *PNAS*, *119*(33), e2202230119. https://doi.org/10.1073/pnas.22022301

Matthews, H. D., & Wynes, S. (2022). Current global efforts are insufficient to limit warming to 1.5°C. *Science*, *376*(6600), 1404–1409. https://doi.org/10.1126/science.abo3378

Mills, M., Visioni, D., & Richter, J. (2022). CESM2 model output CESM2-WACCM6-SSP245 [Dataset]. *NCAR*. https://doi.org/10.26024/0cs0-ev98

Miner, K., Turetsky, M. R., Malina, E., Bartsch, A., Tamminen, J., McGuire, A. D., et al. (2022). Permafrost carbon emissions in a changing Arctic. *Nature Reviews Earth and Environment*, *3*(1), 55–67. https://doi.org/10.1038/s43017-021-00230-3

Morrison, A. L. (2024). Code for "natural variability can mask forced permafrost response to stratospheric aerosol injection in the ARISE-SAI-1.5 simulations [Software]. *Zenodo*. https://doi.org/10.5281/zenodo.10778468

Morrison, A. L., Barnes, E. A., & Hurrell, J. W. (2024). Stratospheric aerosol injection to stabilize northern hemisphere terrestrial permafrost under the ARISE-SAI-1.5 scenario. *Earth's Future*, *12*(4), e2023EF004151. https://doi.org/10.1029/2023EF004151

NASEM. (2021). Reflecting sunlight: Recommendations for solar geoengineering research and research governance (Technical Report). https://doi.org/10.17226/25762

Parazoo, N., Koven, C., Lawrence, D., Romanovsky, V., & Miller, C. (2018). Detecting the permafrost carbon feedback: Talik formation and increased cold-season respiration as precursors to sink-to-source transitions. *The Cryosphere*, *12*(1), 123–144. https://doi.org/10.5194/tc-12-123-2018

Pihl, E., Martin, M., Blome, T., Hebden, S., Jarzebski, M., Lambino, R., et al. (2019). *10 new insights in climate science 2019*. Future Earth & The Earth League.

Rantanen, M., Karpechko, A. Y., Lipponen, A., Nordling, K., Hyvärinen, O., Ruosteenoja, K., et al. (2022). The arctic has warmed nearly four times faster than the globe since 1979. *Communications Earth & Environment*, *3*(168), 4007–4037. https://doi.org/10.1038/s43247-022-00498-3

Riahi, K., van Vuuren, D., Kriegler, E., Edmonds, J., O'Neill, B., Fujimori, S., et al. (2017). The shared socioeconomic pathways and their energy, land use, and greenhouse gas emissions implications: An overview. *Global Environmental Change*, *42*, 153–168. https://doi.org/10.1016/j.gloenvcha.2016.05.009

Richter, J. (2022). CESM2 model output ARISE-SAI-1.5 dataset [Dataset]. *NCAR*. https://doi.org/10.5065/9kcn-9y79

Richter, J., Visioni, D., MacMartin, D., Bailey, D., Rosenbloom, N., Dobbins, B., et al. (2022). Assessing responses and impacts of solar climate intervention on the earth system with stratospheric aerosol injection (ARISE-SAI): Protocol and initial results from the first simulations. *Geoscientific Model Development*, *15*(22), 8221–8243. https://doi.org/10.5194/gmd-15-8221-2022

Ricke, K., Morgan, M., & Allan, M. (2010). Regional climate response to solar-radiation management. *Nature Geoscience*, *15*, 537–541. https://doi.org/10.1038/ngeo915

Schuur, E. A. G., Bockheim, J., Canadell, J. G., Euskirchen, E., Field, C. B., Goryachkin, S. V., et al. (2008). Vulnerability of permafrost carbon to climate change: Implications for the global carbon cycle. *BioScience*, *58*(8), 701–714. https://doi.org/10.1641/b580807

Schuur, E. A. G., McGuire, A. D., Romanovsky, V., Schädel, C., & Mack, M. (2018). Chapter 11: Arctic and boreal carbon. In *Second state of the carbon cycle report (SOCCR2): A sustained assessment report*. U.S. Global Change Research Program. https://doi.org/10.7930/SOCCR2.2018.Ch11

Schuur, E. A. G., McGuire, A. D., Schädel, C., Grosse, G., Harden, J., Hayes, D., et al. (2015). Climate change and the permafrost carbon feedback. *Nature*, *520*(7546), 171–179. https://doi.org/10.1038/nature14338

Smith, R., Jones, P., Briegleb, B., Bryan, F., Danabasoglu, G., Dennis, J., et al. (2010). The Parallel Ocean Program (POP) reference manual: Ocean component of the community climate system model (CCSM) and community earth system model (CESM) [Computer software manual]. *Community Earth System Model*. https://www2.cesm.ucar.edu/models/cesm1.0/pop2/doc/sci/POPRefManual.pdf

Strauss, J., Laboor, S., Schirrmeister, L., Federov, A., Fortier, D., Froese, D., et al. (2021). Circum-Arctic map of the Yedoma permafrost domain. *Frontiers in Earth Science*, *9*, 758360. https://doi.org/10.3389/feart.2021.758360

Strauss, J., Schirrmeister, L., Grosse, G., Fortier, D., Hugelius, G., Knoblauch, C., et al. (2017). Deep Yedoma permafrost: A synthesis of depositional characteristics and carbon vulnerability. *Earth-Science Reviews*, *172*, 75–86. https://doi.org/10.1016/j.earscirev.2017.07.007

Strauss, J., Schirrmeister, L., Grosse, G., Wetterich, S., Ulrich, M., Herzschuh, U., & Hubberten, H.-W. (2013). The deep permafrost carbon pool of the Yedoma region in Siberia and Alaska. *Geophysical Research Letters*, *40*(23), 6165–6170. https://doi.org/10.1002/2013GL058088

Tarnocai, C., Canadell, J., Schuur, E., Kuhry, P., Mazhitova, G., & Zimov, S. (2009). Soil organic carbon pools in the northern circumpolar permafrost region. *Global Biogeochemical Cycles*, *23*(2), GB2023. https://doi.org/10.1029/2008GB003327

Tarnocai, C., Kettles, I. M., & Lacelle, B. (2011). *Peatlands of Canada, open file 6561* [Report]. Geological Survey of Canada. https://doi.org/10.4095/288786

Tilmes, S., Richter, J., Kravitz, B., MacMartin, D., Mills, M., Simpson, I., et al. (2018). CESM1(WACCM) stratospheric aerosol geoengineering large ensemble project. *Bulletin of the American Meteorological Society*, *99*(11), 2361–2371. https://doi.org/10.1175/BAMS-D-17-0267.1

Wells, J., Roberts, D., Lee, P., Cheng, R., & Darveau, M. (2010). *A forest of blue—Canada's boreal forest: The world's waterkeeper*. International Boreal Conservation Campaign.